Math.Comput.Sci. (2014) 8:543–561
DOI 10.1007/s11786-014-0208-7

Mathematics in Computer Science

Sliding Mode Techniques for Robust Trajectory Tracking as well as State and Parameter Estimation

Luise Senkel · Andreas Rauh · Harald Aschemann

Received: 20 December 2013 / Revised: 5 May 2014 / Accepted: 6 June 2014 / Published online: 13 August 2014

Abstract Practical applications are often affected by uncertainties—more precisely bounded and stochastic disturbances. These have to be considered in robust control procedures to prevent a system from being unstable. Common sliding mode control strategies are often not able to cope with the mentioned impacts simultaneously, because they assume that the considered system is only affected by matched uncertainty. Another problem is the offline computation of the switching amplitude. Under these assumptions, important nonlinear system properties cannot be taken into account within the mathematical model of the system. Therefore, this paper presents sliding mode techniques, that on the one hand are able to consider bounded as well as stochastic uncertainties simultaneously, and on the other hand are not limited to the matched case. Firstly, a sliding mode control procedure taking into account both classes of uncertainty is shown. Additionally, a sliding mode observer for the simultaneous estimation of non-measurable system states and uncertain but bounded parameters is described despite stochastic disturbances. This is possible by using intervals for states and parameters in the resulting stochastic differential equations. Therefore, the Itô differential operator is involved and the system's stability can be verified despite uncertainties and disturbances for both control and observer procedures. This operator is used for the online computation of the variable structure part gain (matrix of switching amplitudes) which is advantageous in contrast to common sliding mode procedures.

Keywords Sliding mode control · Sliding mode observer · Parameter estimation · Bounded and stochastic disturbances · Uncertainties · Interval arithmetics

Mathematics Subject Classification 93B12 · 93D09 · 93E15

L. Senkel (✉) · A. Rauh · H. Aschemann
Chair of Mechatronics, University of Rostock, D-18059 Rostock, Germany
e-mail: Luise.Senkel@uni-rostock.de

A. Rauh
e-mail: andreas.rauh@uni-rostock.de

H. Aschemann
e-mail: Harald.Aschemann@uni-rostock.de

1 Introduction

Nonlinearities and several influences such as unknown system parameters, disturbances as well as process and measurement noise make it difficult for researchers to find robust control strategies providing good tracking accuracy and preventing the system from being unstable. The consideration of all these important effects simultaneously is a serious problem in general. Since it is important to control practical applications with high accuracy, mathematical models as well as control and estimation procedures have to be able to cope with the before-mentioned influences. Often, only simplified models can be used in order to apply common control algorithms. Consequently, additional virtual disturbances have to be taken into consideration to account for the neglected nonlinear terms. For the mathematical description of a system, it has to be investigated which effects have an impact on the system dynamics and how these can be taken into consideration. Figure 1 expresses the role of uncertainty in control-oriented modeling: Consider a real system and some corresponding measurements. Inevitably, the mathematical model of the system is only an approximation of the real system since for example nonlinear phenomena (e.g. friction) appear and measurement noise complicates robust control procedures. Nevertheless, the mathematical model is necessary for the design of control strategies requiring knowledge about system parameters and non-measurable system states. The more exact the model represents the real system's properties, the more robust control strategies stabilize the system dynamics in experiment. Therefore, interval algorithms are useful for including bounded uncertainty of states and parameters. Stochastic uncertainty representing noisy measurements or nonlinear system properties is taken into consideration by simulating stochastic differential equations with noise and the corresponding standard deviations. One possibility to deal with these effects is the use of sliding mode procedures which have already been investigated in many publications. In general, one feature of sliding mode procedures is finite-time convergence concerning the reachability of the system's sliding surface. As a consequence, sliding mode control as well as sliding mode observers[1] are able to deal with uncertainties and disturbances [7,18] in a robust and stabilizing way. If the system has reached the sliding surface once, it will not diverge anymore, but it will always stay in the near surrounding area of the sliding surface [17]. Proving Lyapunov stability is an important issue to guarantee robustness of control strategies despite uncertainty as described in [4].

Problems in existing sliding mode procedures are on the one hand chattering phenomena, which can be characterized as high frequency switchings in the control law that make the implementation on a test-rig difficult. On the other hand, the so-called matching conditions represent the requirement that all uncertainties can be compensated by the switching control law only if they enter the state equations in an identical way as the control inputs.

The principle of most sliding mode procedures is as follows: Firstly, a sliding surface that leads the system to an asymptotically stable operation has to be defined. Secondly, using this sliding surface, a suitable candidate of a Lyapunov function is defined (sliding variable for control tasks: difference between desired and actual system states, sliding variable for estimation tasks: difference between actual and estimated system states). As soon as the sliding variable is not equal to zero, the switching amplitude is active and causes the actual states to converge towards with the predefined surface. This strategy is modified in the following description as follows: Control and observer design can be stated as dual problems. For both, the system description is divided into a linear and a nonlinear part. The linear one can be stabilized by e.g. solving linear matrix inequalities, pole placement, linear quadratic regulator approaches etc. The nonlinear part is a variable structure part and is stabilized by an online calculation of the variable structure gain that corresponds to the switching amplitude. Using the Itô differential operator including intervals for parameters as well as for control, estimation, and measurement errors, the switching amplitude can be evaluated. This prevents control and estimation error dynamics from becoming unstable.

This paper is structured as follows. In Sect. 2, basics of sliding mode control and sliding mode estimation are summarized. Based on this, Sect. 3 deals with the extension to nonlinear dynamic systems with bounded and stochastic disturbances. Therefore, the focus is on Lyapunov functions that fulfill two tasks: the calculation of the switching amplitude and a stability proof. An illustrative scenario is described in Sect. 4, for which both the sliding mode controller and observer have been used on the one hand for trajectory tracking and on the other hand for state

[1] In the observer design a joined state and parameter estimation is proposed in this contribution.

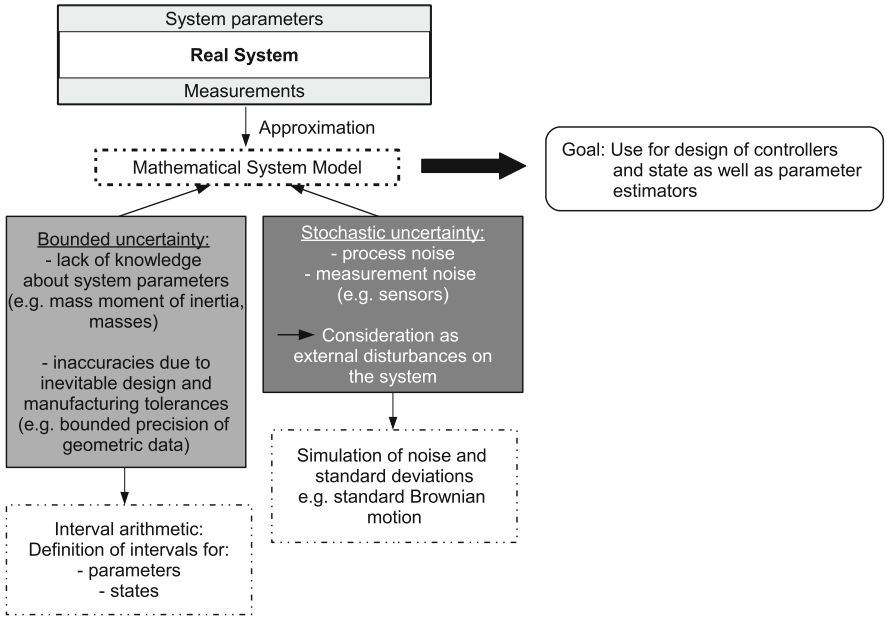

Fig. 1 Relation between different types of uncertainties affecting system models

and parameter estimation simultaneously. Simulation results show the applicability of the described procedures. Finally, conclusions and an outlook on further work are given in Sect. 5.

2 Classical Sliding Mode Control and Observer Design

In recent years, classical as well as higher-order sliding mode control techniques have also been applied for nonlinear dynamic systems [4,22]. The goal is to design tracking control procedures [11] that take into account the system's stability. As it is shown in [5,11], uncertainties can be included in sliding mode techniques using intervals for parameters, disturbances and state deviations. The already mentioned chattering problem especially in the switching control signal can be reduced significantly according to [11], where the control procedure is expanded by an integrator chain at the system input. The result is a smooth control signal, that can alternatively be achieved by using higher-order sliding mode control procedures that are commonly evaluated using nominal values and, hence, without robust interval techniques [16]. The use of higher-order sliding mode techniques then exploits the property that sliding mode techniques are often inherently robust.

As it is described in [7], Lyapunov functions have already been employed for second-order sliding mode algorithms proving finite-time convergence and robustness. In this paper, Lyapunov functions are used for the direct calculation of the switching amplitude in the variable structure control law as well as for the variable structure part of the observer and for the stability proof of the system. The overall goals of the novel interval-based sliding mode control and observer strategies summarized in this paper are to prevent the amplification of measurement noise in parameter estimation tasks to reduce chattering. Chattering commonly leads to an energy-inefficient system operation and to actuator wear.

2.1 Basics of Sliding Mode Control Design

Consider a system that is described by the following set of ODEs

$$\dot{\mathbf{x}}(t) = \mathbf{a}(\mathbf{x}(t)) + \mathbf{B}(\mathbf{x}(t)) \cdot \mathbf{u}(t), \tag{2.1}$$

where $\mathbf{x} \in \mathbb{R}^n$ is the vector of the system states of order n, $\mathbf{u} \in \mathbb{R}^p$ is the vector of the control inputs, $\mathbf{a}(\mathbf{x}(t)) \in \mathbb{R}^n$ is a state-dependent vector, and $\mathbf{B}(\mathbf{x}(t)) \in \mathbb{R}^{n \times p}$ an input matrix. For the sliding mode control of this nonlinear dynamic system, a sliding surface $\mathbf{s}(\tilde{\mathbf{x}}) = \mathbf{0}$ can be defined which characterizes the difference between the system states $\mathbf{x}$ and the desired trajectories $\mathbf{x}_d$. Here, the tracking error is defined according to $\tilde{\mathbf{x}} = \mathbf{x} - \mathbf{x}_d$. The goal of the sliding mode controller is to reach this sliding surface with, in the ideal case, $\tilde{\mathbf{x}} = \mathbf{0}$. Therefore, p switching functions $\mathbf{s}(\tilde{\mathbf{x}}) = [s_1(\tilde{\mathbf{x}}), \ldots, s_p(\tilde{\mathbf{x}})]^T$ are necessary which corresponds to the dimension p of the system input $\mathbf{u}$. Using these p functions, a variable structure control law $\mathbf{u}_s = \left[u_{s,1} \ldots u_{s,p}\right]^T$ with

$$u_{s,i}(\tilde{\mathbf{x}}) = \begin{cases} u_{s,i}^{+}(\tilde{\mathbf{x}}) & \text{for } s_i(\tilde{\mathbf{x}}) > 0 \\ u_{s,i}^{-}(\tilde{\mathbf{x}}) & \text{for } s_i(\tilde{\mathbf{x}}) < 0\,, \quad i = 1, \ldots, p, \end{cases} \tag{2.2}$$

can be obtained [11]. The goal to track the system states to the desired trajectories can be achieved by using the variable structure control law, where the function value of the sliding surface is forced to zero according to $\mathbf{s}(\tilde{\mathbf{x}}) = \mathbf{0}$ (see [11]).

As it can be found in [21,22], the derivative of $\mathbf{s}(\tilde{\mathbf{x}})$ can be computed as

$$\begin{aligned} \dot{\mathbf{s}}(\tilde{\mathbf{x}}) &= \frac{\partial \mathbf{s}}{\partial \tilde{\mathbf{x}}} \cdot \frac{d\tilde{\mathbf{x}}}{dt} = \frac{\partial \mathbf{s}}{\partial \tilde{\mathbf{x}}} \cdot (\dot{\mathbf{x}} - \dot{\mathbf{x}}_d) \\ &= \frac{\partial \mathbf{s}}{\partial \tilde{\mathbf{x}}} \cdot (\mathbf{a}(\mathbf{x}) - \dot{\mathbf{x}}_d) + \frac{\partial \mathbf{s}}{\partial \tilde{\mathbf{x}}} \cdot \mathbf{B}(\mathbf{x}) \cdot \mathbf{u}_{eq}(\tilde{\mathbf{x}}) = \mathbf{0}, \end{aligned} \tag{2.3}$$

where $\dot{\mathbf{s}}(\tilde{\mathbf{x}}) = \mathbf{0}$ holds for perfect trajectory tracking.

Solving this equation for the equivalent control[2] $\mathbf{u}_{eq}(\tilde{\mathbf{x}})$, the system input can be calculated according to

$$\mathbf{u} = \mathbf{u}_{eq}(\tilde{\mathbf{x}}) = -\left(\frac{\partial \mathbf{s}}{\partial \tilde{\mathbf{x}}} \cdot \mathbf{B}(\mathbf{x})\right)^{-1} \cdot \frac{\partial \mathbf{s}}{\partial \tilde{\mathbf{x}}} \cdot (\mathbf{a}(\mathbf{x}) - \dot{\mathbf{x}}_d)\,. \tag{2.4}$$

Now, a quadratic Lyapunov function is taken into consideration according to [11] which aims at the guaranteed stabilization of the switching motion towards the desired trajectory with

$$V(\mathbf{s}) = \frac{1}{2}\,\mathbf{s}^T(\tilde{\mathbf{x}}) \cdot \mathbf{s}(\tilde{\mathbf{x}}) > 0 \quad \text{for} \quad \mathbf{s} \neq \mathbf{0}. \tag{2.5}$$

The time derivative of the Lyapunov function is then given by

$$\dot{V}(\mathbf{s}) = \mathbf{s}^T(\tilde{\mathbf{x}}) \cdot \dot{\mathbf{s}}(\tilde{\mathbf{x}}) \tag{2.6}$$

which guarantees stability if $\dot{V}(\mathbf{s}) < -\eta^T \cdot |\mathbf{s}| < 0$ holds with $\eta_i > 0$ for $i \in \{1, \ldots, p\}$. Moreover, the absolute value $|\mathbf{s}|$ of the switching function is defined component-wise according to

$$|\mathbf{s}| = \operatorname{diag}(\mathbf{s}) \cdot \operatorname{sign}(\mathbf{s}) = \begin{bmatrix} s_1 \cdot \operatorname{sign}(s_1) \\ \vdots \\ s_p \cdot \operatorname{sign}(s_p) \end{bmatrix} \quad \text{with} \quad \operatorname{sign}(s_i) = \begin{cases} +1, & s_i > 0 \\ 0, & s_i = 0\,. \\ -1, & s_i < 0 \end{cases} \tag{2.7}$$

This control procedure is not only defined for nominal values of system parameters and (measured) states. In fact, it can be extended to intervals for system parameters and control errors as it is also shown in [11]. The advantage of this extension is, that chattering can be reduced and the system's stability can be guaranteed in spite of uncertain parameters and measurement errors or external and bounded disturbances.

[2] Assumption: the product $\frac{\partial \mathbf{s}}{\partial \tilde{\mathbf{x}}} \cdot \mathbf{B}(\mathbf{x})$ is regular. The equivalent control represents the system input for states that are located on $\mathbf{s}(\tilde{\mathbf{x}}) = \mathbf{0}$.

2.2 Classical Sliding Mode Observer Design

Assume that a dynamic system can be represented by $\dot{\mathbf{x}}(t) = \mathbf{f}(\mathbf{x}(t), \mathbf{u}(t))$ with the set of state equations

$$\begin{aligned} \dot{\mathbf{x}}(t) &= \mathbf{A} \cdot \mathbf{x}(t) + \mathbf{B} \cdot \mathbf{u}(t) + \mathbf{S} \cdot \xi(\mathbf{x}(t), \mathbf{u}(t)) \\ \mathbf{y}(t) &= \mathbf{C} \cdot \mathbf{x}(t) . \end{aligned} \tag{2.8}$$

In (2.8), the state vector $\mathbf{x}(t)$—which includes also uncertain but bounded parameters $\mathbf{p}(t) \in [\mathbf{p}(t)]$—constant system, input and output matrices $\mathbf{A}$, $\mathbf{B}$ as well as $\mathbf{C}$ and the control input vector $\mathbf{u}(t)$ are considered. All nonlinear terms, that do not fit into this linear formulation, and the influence of a-priori unknown terms on the system dynamics are represented in the matrix $\mathbf{S} \in \mathbb{R}^{n \times q}$ with the condition $\|\xi(\mathbf{x}, \mathbf{u})\| \leq \overline{\xi}$ and a fixed upper bound on the vector norm $\overline{\xi}$.

For this system, a dual problem to sliding mode control can be formulated, with the following set of ODEs representing a variable structure observer [6] according to

$$\dot{\hat{\mathbf{x}}}(t) = \hat{\mathbf{A}} \cdot \hat{\mathbf{x}}(t) + \hat{\mathbf{B}} \cdot \mathbf{u}(t) + h_s \cdot \mathbf{S} \cdot \tilde{\mathbf{e}} + \mathbf{H}_p \cdot \Big(\mathbf{y}_m(t) - \hat{\mathbf{C}} \cdot \hat{\mathbf{x}}(t)\Big). \tag{2.9}$$

In Eq. (2.9), $\hat{\mathbf{A}}$, $\hat{\mathbf{B}}$ and $\hat{\mathbf{C}}$ denote the system, input and output matrices of the observer parallel model where it is assumed that these matrices are known. Moreover, h_s is the scaling factor for the variable structure part. To guarantee asymptotic stability, this term has to be chosen such that nonlinearities and uncertainties do not destabilize the system [16]. To stabilize the error dynamics of the linear part, the observer gain matrix $\mathbf{H}_p$ is taken into consideration. There are several possibilities for choosing this matrix, e.g. by pole assignment, linear matrix inequalities, or minimizing a quadratic cost function as it is shown in [13,17]. The vector $\mathbf{y}_m(t)$ contains all measured system outputs. The error vector defined by $\tilde{\mathbf{e}} := \frac{\mathbf{S}^T \mathbf{P}(\mathbf{x}-\hat{\mathbf{x}})}{\|\mathbf{S}^T \mathbf{P}(\mathbf{x}-\hat{\mathbf{x}})\|}$ accounts for deviations between the true and estimated system states [16]. The matrix $\mathbf{P}$ results from solving the Lyapunov equation $\mathbf{A}_O \cdot \mathbf{P} + \mathbf{P} \cdot \mathbf{A}_O^T + \mathbf{Q} = \mathbf{0}$ with the matrix $\mathbf{A}_O = \hat{\mathbf{A}} - \mathbf{H}_p \cdot \hat{\mathbf{C}}$ of the linear observer part. Note, that the pair $(\hat{\mathbf{A}}, \hat{\mathbf{C}})$ has to be observable, otherwise the described procedure is not applicable to the given system. Another requirement is, that all terms included in the product $\mathbf{S} \cdot \xi(\mathbf{x}(t), \mathbf{u}(t))$ have to be bounded.

Equation (2.9) can be adapted, as soon as a change of sign occurs in the difference between the true and estimated states. Then, the term ξ in (2.8) can be reproduced approximately by $\tilde{\mathbf{e}}$ in the switching part of the observer [16]. Therefore, the observer differential equation is changed into

$$\dot{\hat{\mathbf{x}}}(t) = \hat{\mathbf{A}} \cdot \hat{\mathbf{x}}(t) + \hat{\mathbf{B}} \cdot \mathbf{u}(t) + \mathbf{H}_p \cdot \mathbf{e}_m(t) + h_s \cdot \tilde{\mathbf{S}} \cdot \operatorname{sign}(\mathbf{e}_m(t)) \tag{2.10}$$

with $\mathbf{e}_m(t) = \mathbf{y}_m(t) - \mathbf{C} \cdot \hat{\mathbf{x}}(t)$. Equation (2.10) consists of a locally valid linear system model as well as of the variable structure term that makes it possible to handle uncertainty and nonlinearities without destabilizing the error dynamics [16]. In this context, the disadvantage of common sliding mode estimation schemes is the need to define the switching amplitude h_s a-priori. This often leads to unnecessarily large chattering and—in the case of including the observer in a closed-loop control structure—to a deterioration of the quality of the control signal.

3 Sliding Mode Control and Estimation Using Intervals

The presented procedures for sliding mode control and estimation can be extended such that uncertain parameters can be considered instead of their nominal values during design and implementation. As shown in [5,11], uncertainty in parameters and measured system states can be treated by means of interval arithmetic [8]. In addition, process and measurement noise that simulate for example inaccurate sensor measurements in real applications, can be included

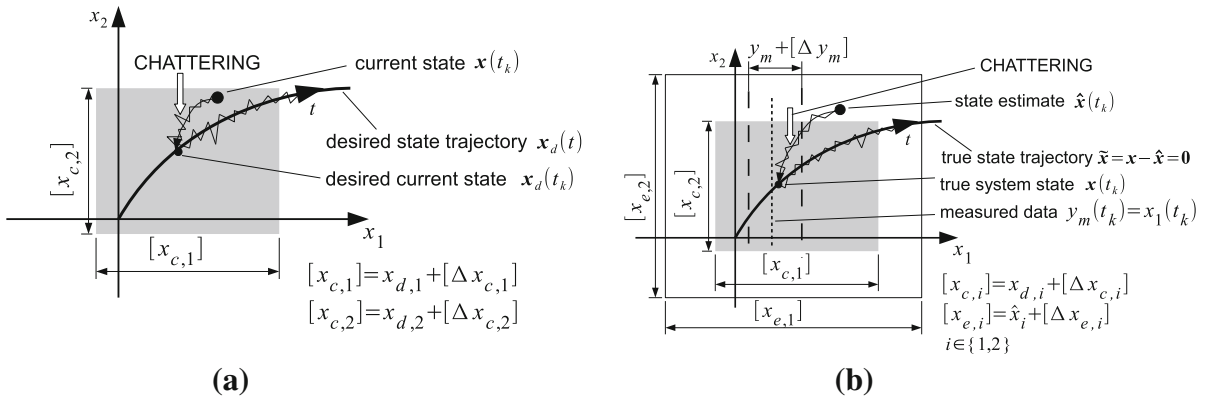

Fig. 2 Location of intervals for the sliding mode control and sliding mode observer. **a** Interval definitions for control design, **b** interval definitions for observer design

to increase the robustness of the algorithms presented in the following. To verify asymptotic stability, the negative definiteness of the time derivative of a suitable candidate of a Lyapunov function can be exploited. The goal of the interval extension is to reduce the switching amplitudes of the variable structure control and observer approaches. In such a way, the two before-mentioned issues chattering and actuator wear can be reduced efficiently. In [16], a novel sliding mode-type observer is presented that includes uncertainty of system parameters, interval specifications for control inputs, and intervals for estimation and measurement errors. On this basis, the procedure presented in this paper estimates states and parameters simultaneously although they are coupled in a multiplicative way. The estimation of parameters is especially useful in cases, in which system parameters are not constant, e.g. friction coefficients or mass moments of inertia. This is the basis for the presented extension of the sliding mode observer that is further generalized to consider stochastic process and measurement noise. Before these improved control and observer approaches are described, firstly, basics for interval arithmetic and secondly, linear matrix inequalities for an underlying stabilization of the sliding mode approaches are summarized.

3.1 Interval Arithmetics

The use of intervals is reasonable if at least one of the following influence factors affects the system, namely

- bounded uncertainties: e.g. unknown system parameters,
- bounded accuracy of measurements, and
- bounded nonlinearities affecting the system dynamics.

To get an impression of the use of intervals for both the sliding mode controller and observer presented in the following, Fig. 2 shows the location of the considered intervals for control, estimation and measurement errors ($[\Delta x_c]$, $[\Delta x_e]$ and $[\Delta y_m]$, resp.) as boxes.

Furthermore, it is assumed that the true parameter values are unknown. This corresponds to real systems since—exemplarily in mechatronic applications—even lengths, masses and friction coefficients are never exactly known. In the following, intervals in general are defined by $[\kappa] := [\underline{\kappa}; \overline{\kappa}] = [\inf([\kappa]); \sup([\kappa])]$ with the infimum $\underline{\kappa} = \inf([\kappa])$ which denotes the lower bound and the supremum $\overline{\kappa} = \sup([\kappa])$ which denotes the upper bound. For vector-valued intervals, this definition holds individually for each component of the vector.

3.2 Linear Matrix Inequalities for the Design of a Robust Linear Controller

Linear Matrix Inequalities (LMIs) [2,3] can be used for a robust control and observer design of the linear system part, because their appropriate use guarantees asymptotic stability for bounded parameter intervals.

Assume the state-space representation of a dynamic system according to

$$\begin{aligned}\dot{\mathbf{x}}(t) &= \mathbf{f}(\mathbf{x}(t), [\mathbf{p}], \mathbf{u}(t)) := \mathbf{A}_C(\mathbf{x}(t), [\mathbf{p}]) \cdot \mathbf{x}(t) + \mathbf{B}_C(\mathbf{x}, [\mathbf{p}]) \cdot \mathbf{u}(t) \\ \mathbf{y}(t) &= \mathbf{C}_C(\mathbf{x}(t), [\mathbf{p}]) \cdot \mathbf{x}(t)\end{aligned} \tag{3.1}$$

with an element-wise defined interval parameter vector $[\mathbf{p}]$. Additionally, the desired operating point is defined as $\mathbf{x} = \mathbf{0}$ which is supposed to be stabilized using the feedback control law $\mathbf{u}(t) = -\mathbf{K} \cdot \mathbf{x}(t)$. Note, that all system states have to be observable or measurable.

As shown in [12], uncertain but bounded parameters $\mathbf{p}$ can be handled for a system $\dot{\mathbf{x}}(t) = \mathbf{f}(\mathbf{x}(t, [\mathbf{p}], \mathbf{u}(t))$ such that their influence is over-approximated by the polytopic domain $\mathcal{D}$, with the following convex combination (linear in ψ_v)

$$\mathcal{D} = \left\{ [\mathbb{A}_C, \mathbb{B}_C, \mathbb{C}_C] \middle| [\mathbb{A}_C, \mathbb{B}_C, \mathbb{C}_C] = \sum_{v=1}^{n_v} \psi_v \cdot \left[\mathbf{A}_{C,v}, \mathbf{B}_{C,v}, \mathbf{C}_{C,v}\right]; \sum_{v=1}^{n_v} \psi_v = 1; \psi_v \geq 0 \right\} \tag{3.2}$$

of the interval expressions of the system matrix $\mathbb{A}_C := \mathbf{A}_C(\psi)$, control matrix $\mathbb{B}_C := \mathbf{B}_C(\psi)$, and output matrix $\mathbb{C}_C := \mathbf{C}_C(\psi)$, where ψ denotes the dependency of $\mathbb{A}_C$, $\mathbb{B}_C$ and $\mathbb{C}_C$ on the parameters $\mathbf{p}$ and states $\mathbf{x}$. In $\mathcal{D}$, all possible parameter configurations are included and specified by their lower and upper bounds. The corresponding n_v matrix vertices are $\mathbf{A}_{C,v} := \mathbf{A}_{C,v}(\mathbf{x}, \mathbf{p}) \in \mathbb{A}_C([\mathbf{x}], [\mathbf{p}])$, $\mathbf{B}_{C,v} := \mathbf{B}_{C,v}(\mathbf{x}, \mathbf{p}) \in \mathbb{B}_C([\mathbf{x}], [\mathbf{p}])$ and $\mathbf{C}_{C,v} := \mathbf{C}_C(\mathbf{x}, \mathbf{p}) \in \mathbb{C}_C([\mathbf{x}], [\mathbf{p}])$. The goal is to find the control gain matrices $\mathbf{K}$ and $\mathbf{P}_C$ using LMIs such that stability is guaranteed for every parameter located in the respective intervals.

A suitable candidate of a Lyapunov function is given by $V_C = \frac{1}{2}\mathbf{x}^T(t)\,\mathbf{P}_C\mathbf{x}(t)$ with the positive definite matrix $\mathbf{P}_C = \mathbf{P}_C^T \succ 0$ [17]. Its time derivative follows as

$$\dot{V}_C(\mathbf{x}) = \frac{1}{2}\dot{\mathbf{x}}^T \cdot \mathbf{P}_C \cdot \mathbf{x} + \frac{1}{2}\mathbf{x}^T \cdot \mathbf{P}_C \cdot \dot{\mathbf{x}} = \frac{1}{2}\mathbf{x}^T \cdot \left[\tilde{\mathbf{A}}_C^T \cdot \mathbf{P}_C + \mathbf{P}_C \cdot \tilde{\mathbf{A}}_C\right] \cdot \mathbf{x} \prec 0 \tag{3.3}$$

with $\tilde{\mathbf{A}}_C = \mathbb{A}_C - \mathbb{B}_C\mathbf{K}$ (time arguments omitted). The term $\tilde{\mathbf{A}}_C^T \cdot \mathbf{P}_C + \mathbf{P}_C \cdot \tilde{\mathbf{A}}_C \prec 0$ forms a bilinear matrix inequality (BMI), that can be reformulated by a multiplication with $\mathbf{P}_C^{-1}$ from the left and right-hand sides. Including the polytopic uncertainty according to Eq. (3.2), the following BMI

$$\left(\mathbf{A}_{C,v} - \mathbf{B}_{C,v}\mathbf{K}\right)^T \cdot \mathbf{P}_C + \mathbf{P}_C \cdot \left(\mathbf{A}_{C,v} - \mathbf{B}_{C,v}\mathbf{K}\right) + 2\gamma_C\mathbf{P}_C \prec 0 \tag{3.4}$$

holds with a minimum convergence rate $\gamma_C > 0$. In the case of, for example, two interval variables, $n_v = 2^2 = 4$ LMIs have to be considered that contain the complete ranges defined in $\mathcal{D}$. A linearizing change of variables (related to the left and right multiplication with $\mathbf{P}_C^{-1}$) leads to

$$\mathbf{Q}_C\mathbf{A}_{C,v}^T - \mathbf{Y}_C^T\mathbf{B}_{C,v}^T + \mathbf{A}_{C,v}\mathbf{Q}_C - \mathbf{B}_{C,v}\mathbf{Y}_C + 2\gamma_C\mathbf{Q}_C \prec 0 \tag{3.5}$$

with $\mathbf{P}_C = \mathbf{Q}_C^{-1}$ and $\mathbf{K} = \mathbf{Y}_C\mathbf{P}_C$ for all $v \in \{1, ..., n_v\}$. Functionalities for computing with interval arithmetics that are necessary for range computations in the matrices in (3.2) are obtained with the interval toolbox IntLab [14]. The n_v matrix inequalities (3.5) are solved simultaneously by means of SeDuMi [19] in combination with YALMIP [10] in MATLAB such that $\mathbf{Q}_C$ and $\mathbf{Y}_C$ stabilize the system for all parameter values inside the intervals $[\mathbf{p}]$. The approach of an LMI-based robust system stabilization is also applicable to the observer design as it has been shown in [17]. Then, the observer gain matrices $\mathbf{H}_p$ and $\mathbf{P}_O$ are calculated using LMIs.

3.3 Interval Sliding Mode Control (ISMC)

In this section, an extension of the classical sliding mode control (see Sect. 2.1) to an interval-based approach is described, as it can be found in [17]. The goal is to avoid the problem that the results become too conservative in case of uncertain parameters. As a consequence, large switching amplitudes and actuator wear can be reduced by the presented novel approach [11].

Consider the uncertain system of order n (for more information about the classical notation of nonlinear stochastic differential equations refer to [1])

$$d\mathbf{x} = \mathbf{f}(\mathbf{x}(t), [\mathbf{p}], \mathbf{u}(t))dt + \mathbf{G}_p \, d\mathbf{w}_p \tag{3.6}$$

$$\mathbf{y} = \mathbb{C}_C(\mathbf{x}(t), [\mathbf{p}]) \cdot \mathbf{x}(t) + \mathbf{G}_m \, d\mathbf{w}_m \tag{3.7}$$

with

$$\mathbf{f}(\mathbf{x}(t), [\mathbf{p}], \mathbf{u}(t)) = \mathbb{A}_C(\mathbf{x}(t), [\mathbf{p}]) \cdot \mathbf{x}(t) + \mathbb{B}_C(\mathbf{x}(t), [\mathbf{p}]) \cdot \mathbf{u}(t) \ , \tag{3.8}$$

the standard Brownian motions of the process noise $d\mathbf{w}_p \in \mathbb{R}^{r_p}$ and of the measurement noise $d\mathbf{w}_m \in \mathbb{R}^{r_m}$. Moreover, $\mathbb{A}_C(\mathbf{x}(t), [\mathbf{p}])$, $\mathbb{B}_C(\mathbf{x}(t), [\mathbf{p}])$ and $\mathbb{C}_C(\mathbf{x}(t), [\mathbf{p}])$ are the interval expressions of the system, input and output matrices in which intervals for all system parameters are included. Additionally, the stochastic noise terms are characterized by the standard deviations $\mathbf{G}_p \in \mathbb{R}^{n \times r_p}$ and $\mathbf{G}_m \in \mathbb{R}^{n_y \times r_m}$. Note, that the linear formulation of $\mathbf{f}(\mathbf{x}(t), [\mathbf{p}], \mathbf{u}(t))$ in Eq. (3.8) is not required but in this context assumed with regard to the application scenario in Sect. 4. Moreover, in Eqs. (3.6) and (3.8), the control law consists of a static or dynamic feed-forward control $\mathbf{u}_V$, a state feedback and a switching part according to

$$\mathbf{u}(t) = \mathbf{u}_V(t) - \mathbf{K} \cdot \mathbf{x}(t) + \eta \cdot \text{sign}(\mathbf{x}(t) - \mathbf{x}_d(t)) \tag{3.9}$$

with the vector of desired trajectories $\mathbf{x}_d(t)$. Note, that η is a matrix of all switching amplitudes in the general case. For $u \in \mathbb{R}$, $\mathbf{x} \in \mathbb{R}^n$, the matrix η becomes a row vector according to $\eta \in \mathbb{R}^{1 \times n}$. This variable structure part gain η stabilizes the nonlinear part. The matrix $\mathbf{K}$ can be either calculated by pole assignment for one working point defined by using LMIs (see Sect. 3.2) or by one special parameter configuration in $\mathcal{D}$ to guarantee underlying robust stability of the linear part of the system.

3.3.1 Calculation of the Switching Amplitude

Since stochastic disturbances are taken into consideration, the Itô differential operator [9] is used for the calculation of switching amplitudes according to the following procedure. In this approach, the Itô differential operator serves as a substitute for the deterministic time derivative of the Lyapunov function V_C with

$$L(V_C(t)) = \frac{\partial V_C}{\partial t} + \left(\frac{\partial V_C}{\partial \tilde{\mathbf{x}}}\right)^T \cdot (\mathbf{f}(\mathbf{x}(t), [\mathbf{p}], \mathbf{u}(t)) - \dot{\mathbf{x}}_d(t)) + \frac{1}{2}\text{trace}\left\{\mathbf{G}_p^T \frac{\partial^2 V_C}{\partial \tilde{\mathbf{x}}^2}\mathbf{G}_p\right\}. \tag{3.10}$$

For guaranteed stability of Eq. (3.10), a suitable candidate for a Lyapunov function

$$V_C = \frac{1}{2}\tilde{\mathbf{x}}^T(t)\mathbf{P}_C\tilde{\mathbf{x}}(t) \tag{3.11}$$

is defined with the difference between the actual and desired system states according to $\tilde{\mathbf{x}} = \mathbf{x} - \mathbf{x}_d = [x_1 - x_{1,d}, \ x_2 - x_{2,d}, \ \ldots, x_n - x_{n,d}]^T$ (time-arguments are omitted). Since there is no explicit dependency of the Lyapunov function on the time t, the condition $\frac{\partial V_C}{\partial t} = 0$ holds in Eq. (3.10). In case that no stochastic processes are taken into account, $\mathbf{G}_p = \mathbf{0}$ holds. For a guaranteed stability proof, the condition $L(V_C(t)) \overset{!}{<} 0$ needs to be fulfilled which corresponds to $\dot{V}_C < 0$. Instead of this, the condition $L(V_C(t)) \overset{!}{<} -\mathbf{q}_C^T \text{abs}([\tilde{\mathbf{x}}])$ with an additionally user-defined convergence rate vector $\mathbf{q}_C$ can be demanded. Here, it is assumed that $\mathbf{q}_C$ is a component-wise non-negative vector. After substituting all terms, the components $i \in \{1, \ldots, n\}$ of the switching amplitude vector in the single-input single-output (SISO) case are calculated by

$$\eta_i = \begin{cases} 0, & \text{if } [\delta_C] \subseteq (\mathbb{B}_C^T\mathbf{P}_C \, |[\tilde{\mathbf{x}}]|)_i \\ \sup\left((\mathbb{B}_C{}^T\mathbf{P}_C \, |[\tilde{\mathbf{x}}]|)_i^+ \cdot \left(-[\dot{V}_{a,C}] - \mathbf{q}_C^T \text{abs}\,([\tilde{\mathbf{x}}]) - T\right)\right), & \text{for } \sup(\mathbb{B}_C^T\mathbf{P}_C \, |[\tilde{\mathbf{x}}]|)_i < 0 \\ \inf\left((\mathbb{B}_C{}^T\mathbf{P}_C \, |[\tilde{\mathbf{x}}]|)_i^+ \cdot \left(-[\dot{V}_{a,C}] - \mathbf{q}_C^T \text{abs}\,([\tilde{\mathbf{x}}]) - T\right)\right), & \text{for } \inf(\mathbb{B}_C^T\mathbf{P}_C \, |[\tilde{\mathbf{x}}]|)_i > 0 \end{cases} \tag{3.12}$$

with the vector of absolute values of the difference between the system states and the desired trajectories according to

$$\text{abs}\,([\tilde{\mathbf{x}}]) = \begin{bmatrix} \text{abs}([x_1] - x_{1,d}) \\ \vdots \\ \text{abs}([x_n] - x_{n,d}) \end{bmatrix} \quad \text{with} \quad \text{abs}\ ([\tilde{x}_i]) = \begin{cases} \left[-\overline{\tilde{x}}_i\ ;\ -\underline{\tilde{x}}_i\right] & \text{for } \overline{\tilde{x}}_i \leq 0 \\ \left[\underline{\tilde{x}}_i\ ;\ \overline{\tilde{x}}_i\right] & \text{for } \underline{\tilde{x}}_i \geq 0 \\ \left[0\ ;\ \max\{|\underline{\tilde{x}}_i|, |\overline{\tilde{x}}_i|\}\right] & \text{else.} \end{cases} \tag{3.13}$$

The function `abs` is provided by the C++ library C-XSC. In Eq. (3.12), the time derivative of the continuous part of the Lyapunov function follows to

$$[\dot{V}_{a,C}] = [\tilde{\mathbf{x}}]^T \mathbf{P}_C (\mathbb{A}_C - \mathbb{B}_C \mathbf{K}) \cdot [\mathbf{x}] + [\tilde{\mathbf{x}}]^T \mathbf{P}_C \mathbb{B}_C \mathbf{u}_V - [\tilde{\mathbf{x}}]^T \mathbf{P}_C \dot{\mathbf{x}}_d \tag{3.14}$$

and the term

$$T = \frac{1}{2} \text{trace} \left\{ \mathbf{G}_p^T \frac{\partial^2 V_C}{\partial \tilde{\mathbf{x}}^2} \mathbf{G}_p \right\}. \tag{3.15}$$

Moreover, Eq. (3.12) also includes $\mathbb{A}_C$ and $\mathbb{B}_C$ which denote the interval evaluations of $\mathbf{A}_C(\mathbf{x}, [\mathbf{p}])$ and $\mathbf{B}_C(\mathbf{x}, [\mathbf{p}])$ at each point of time t. In the multi-input multi-output case, the components in (3.12) form the rows of the switching amplitude matrix. Moreover, a small interval $[\delta_C]$ defining a tight area around zero (element-wise) prevents the sliding mode controller from switching around $\tilde{\mathbf{x}} = \mathbf{0} + [\delta_C]$. The reason for this choice is that in the corresponding regions it cannot be determined whether $\tilde{\mathbf{x}}(t) = \mathbf{x}_d(t) - \hat{\mathbf{x}}(t) < 0$ or $\tilde{\mathbf{x}}(t) = \mathbf{x}_d(t) - \hat{\mathbf{x}}(t) > 0$ hold component-wise [17]. Nevertheless, this knowledge is necessary for the calculation of the switching amplitude. Moreover, the chattering phenomenon inevitably occurs if the sliding surface is reached. To reduce this problem and to ensure finite-time convergence, the interval $[\delta_C]$ effects the calculation of smaller switching amplitudes in the near surrounding area of the sliding surface. This feature can be understood as a compromise between chattering phenomena and finite-time convergence. Note, high switching amplitudes in the control law in real applications may cause wear of the system.

The left pseudo inverse of the interval expression $[\mathbf{M}] := (\mathbb{B}_C^T \mathbf{P}_C |[\tilde{\mathbf{x}}]|)$, $\mathbf{M} \in \mathbb{R}^{n_1 \times n_2}$ is calculated by an interval Newton method using the function `inv` from the C++ library C-XSC [20] according to

$$[\mathbf{M}]^+ = \begin{cases} [\mathbf{M}]^{-1} & \text{if } [\mathbf{M}] \text{ is scalar} \\ ([\mathbf{M}]^T [\mathbf{M}])^{-1} [\mathbf{M}]^T & \text{if } n_1 \geq n_2 \\ \left(([\mathbf{M}][\mathbf{M}]^T)^{-1} [\mathbf{M}]\right)^T & \text{if } n_1 < n_2\,. \end{cases} \tag{3.16}$$

The pseudo inverse $[\mathbf{M}]^+$ for the following scenario is always of full rank despite uncertainty. In (3.12), the interval matrix of the absolute values $|[\tilde{\mathbf{x}}]| \in \mathbb{R}^{n \times n}$ with the interval around the sliding surface $[\tilde{x}_i] = ([x_i] - x_{i,d})$ is defined as

$$|[\tilde{\mathbf{x}}]| = \begin{bmatrix} [\tilde{x}_1] \cdot \text{sign}([\tilde{x}_1]) & [\tilde{x}_1] \cdot \text{sign}([\tilde{x}_2]) & \dots & [\tilde{x}_1] \cdot \text{sign}([\tilde{x}_n]) \\ [\tilde{x}_2] \cdot \text{sign}([\tilde{x}_1]) & [\tilde{x}_2] \cdot \text{sign}([\tilde{x}_2]) & \dots & [\tilde{x}_2] \cdot \text{sign}([\tilde{x}_n]) \\ \vdots & \vdots & \ddots & \vdots \\ [\tilde{x}_n] \cdot \text{sign}([\tilde{x}_1]) & [\tilde{x}_n] \cdot \text{sign}([\tilde{x}_2]) & \dots & [\tilde{x}_n] \cdot \text{sign}([\tilde{x}_n]) \end{bmatrix} \tag{3.17}$$

which is evaluated for all vector components $i \in \{1, ..., n\}$ and the sign function of an interval according to

$$\text{sign}([\tilde{x}_i]) = \begin{cases} 1 & \text{if} \quad \inf([\tilde{x}_i]) = (\inf([x_i]) - x_{i,d}) > 0 \\ -1 & \text{if} \quad \sup([\tilde{x}_i]) = (\sup([x_i]) - x_{i,d}) < 0 \\ 0 & \text{else.} \end{cases} \tag{3.18}$$

So far, it has been assumed, that all system states are known by measurements. In reality, however, this is not the case, so the states have to be estimated. Then, in the control law $\mathbf{u}(t) = \mathbf{u}_V(t) - \mathbf{K} \cdot \hat{\mathbf{x}}(t) + \eta \cdot \text{sign}\,(\mathbf{x}_d(t) - \hat{\mathbf{x}}(t))$ and for all equations in Sect. 3.3.1, the state vector $\mathbf{x}(t)$ is replaced by the estimated state vector $\hat{\mathbf{x}}(t)$ according to the new definition of the sliding surface $\tilde{\mathbf{x}}(t) = \mathbf{x}_d(t) - \hat{\mathbf{x}}(t)$. Additionally, it is assumed that the actual state vector is unknown and that the estimated state vector may not fully coincide with $\mathbf{x}(t)$. Hence, the state vector is extended by the control error interval $[\Delta\mathbf{x}_c]$ according to $\mathbf{x}(t) \in [\mathbf{x}] := \mathbf{x}(t) + [\Delta\mathbf{x}_c]$ and the estimated state vector by the estimation error interval $[\Delta\mathbf{x}_e]$ according to $\hat{\mathbf{x}}(t) \in \left[\hat{\mathbf{x}}\right] := \hat{\mathbf{x}}(t) + [\Delta\mathbf{x}_e]$ (both element-wise). To sum up, the presented procedure provides the possibility to calculate the switching amplitude online in every time step considering uncertainty of parameters and states. The same holds for the following sliding mode observer in Sect. 3.4. which aims at the estimation of all system states and parameters despite stochastic disturbances as the dual problem of the controller described above.

3.3.2 Boundary of the Provable Stability Domain

To prove whether the system is asymptotically stable, $L(V_C)$ needs to be evaluated with the calculated switching control law; if $L(V_C(t)) < 0$, the system is stable. Note, that the stability boundary $L(V_C(t)) = 0$ is commonly shaped like an ellipsoid around the desired operating point whose volume should be as small as possible to reduce the non-stabilizable area. The ellipsoid-like shape results from the stochastic disturbance included in T. This disturbance reduces the provable stability domain according to [13].

3.4 Interval Sliding Mode Observer (ISMO)

The classical sliding mode observer in Sect. 2.2 can be modified in analogy to the control task in the previous subsection to a robust interval approach. In contrast to the sliding mode controller, for which the number of switching amplitudes in the control law is equal to the system order, the interval sliding mode observer possesses as many switching amplitudes in the variable structure part as measurements of states are available. Here, the Lyapunov function candidate is chosen as $V_O = \frac{1}{2}\mathbf{e}^T(t)\mathbf{P}_O\mathbf{e}(t)$ with the error $\mathbf{e}(t) = \mathbf{x}(t) - \hat{\mathbf{x}}(t)$ between the true and estimated system states. For the consideration of stochastic disturbances, again the Itô differential operator

$$L(V_O(t)) = \frac{\partial V_O}{\partial t} + \left(\frac{\partial V_O}{\partial \mathbf{e}}\right)^T \cdot \left(\mathbf{f}(\mathbf{x}\,(t)\,, [\mathbf{p}], \mathbf{u}\,(t)) - \hat{\hat{\mathbf{f}}}(\hat{\mathbf{x}}(t), [\mathbf{p}], \mathbf{u}\,(t))\right) + \frac{1}{2}\text{trace}\left\{\mathbf{G}^T \frac{\partial^2 V_O}{\partial \mathbf{e}^2}\mathbf{G}\right\} \tag{3.19}$$

is used under consideration of Eq. (3.1), where the term $\hat{\hat{\mathbf{f}}}(\hat{\mathbf{x}}\,(t)\,, [\mathbf{p}], \mathbf{u}(t))$ and the corresponding output equation are defined as

$$\begin{aligned}
\hat{\hat{\mathbf{f}}}(\hat{\mathbf{x}}\,(t)\,, [\mathbf{p}], \mathbf{u}(t)) &= \hat{\mathbf{f}}(\mathbf{x}\,(t)\,, [\mathbf{p}], \mathbf{u}(t)) + \mathbf{P}_O^{+}\mathbb{C}_O^T(\hat{\mathbf{x}}\,(t)\,, [\mathbf{p}]) \cdot \mathbf{H}_s \cdot \text{sign}(\mathbf{e}_m + [\Delta\mathbf{y}_m]) \\
&:= \mathbb{A}_O(\hat{\mathbf{x}}\,(t)\,, [\mathbf{p}]) \cdot \hat{\mathbf{x}}\,(t) + \mathbb{B}_O(\hat{\mathbf{x}}\,(t)\,, [\mathbf{p}]) \cdot \mathbf{u}\,(t) + \mathbf{H}_p \cdot [\mathbf{e}_m] \\
&\quad + \mathbf{P}_O^{+}\mathbb{C}_O^T(\hat{\mathbf{x}}\,(t)\,, [\mathbf{p}]) \cdot \mathbf{H}_s \cdot \text{sign}(\mathbf{e}_m + [\Delta\mathbf{y}_m]) \qquad (3.20) \\
\hat{\mathbf{y}}_m &:= \mathbb{C}_O(\hat{\mathbf{x}}\,(t)\,, [\mathbf{p}]) \cdot \hat{\mathbf{x}}\,(t) \qquad (3.21)
\end{aligned}$$

with the component-wise defined measurement error interval vector $\mathbf{e}_m(t) \in [\mathbf{e}_m]$ and the interval matrices $\mathbb{A}_O$, $\mathbb{B}_O$ and $\mathbb{C}_O$ denoting the interval evaluations of $\mathbf{A}_O(\hat{\mathbf{x}}\,(t)\,, [\mathbf{p}])$, $\mathbf{B}_O(\hat{\mathbf{x}}\,(t)\,, [\mathbf{p}])$ and $\mathbf{C}_O(\hat{\mathbf{x}}\,(t)\,, [\mathbf{p}])$, resp. The error interval $[\mathbf{e}_m]$ accounts for deviations due to bounded uncertainty between the measured and estimated system outputs with $[\mathbf{e}_m] = \mathbf{y}_m(t) - \hat{\mathbf{y}}_m(t) + [\Delta\mathbf{y}_m]$. Moreover, the matrix $\mathbf{G}$ contains the standard deviation of both process as well as measurement noise according to $\mathbf{G} = [\mathbf{G}_p, -\mathbf{H}_p\mathbf{G}_m]$ in combination with the observer gain $\mathbf{H}_p$ of the linear part.

As for the sliding mode control, where the system states are assumed to follow desired trajectories, the estimated states of the observer should coincide with the corresponding true ones: here, an estimation error interval $[\Delta\mathbf{x}_e]$ is included to prevent the observer from switching in regions near zero, where the positive or negative sign of $\mathbf{e}_m$ cannot be determined, see [16]. The underlying stabilizing observer gain $\mathbf{H}_p$ and the matrix $\mathbf{P}_O$ in $\hat{\tilde{\mathbf{f}}}$ can be calculated by pole assignment, minimizing a quadratic cost function or by LMIs.

The advantage of using LMIs, for control and estimation tasks, is the calculation of matrices $\mathbf{H}_p$, $\mathbf{K}$, $\mathbf{P}_C$, and $\mathbf{P}_O$ that guarantee stability for parameter intervals whereas—for pole assignment—point values are necessary for the system, input, and output matrices. Hence, the gains obtained by pole assignment do not necessarily guarantee robust stability for large operating regions of the system without the variable structure part.

The switching amplitude of the sliding mode observer which accounts for interval variables and stochastic disturbances, can be calculated by a user-defined stability margin $\mathbf{q}_O$ (element-wise non-negative) with

$$L(V_O(t)) \overset{!}{<} -\mathbf{q}_O^T \left|[\mathbf{e}_m]\right| . \tag{3.22}$$

Then, the switching amplitude matrix $\mathbf{H}_s$ follows as a diagonal matrix from the vector of switching amplitudes according to $\mathbf{H}_s = \mathrm{diag}(\mathbf{h}_s) \in \mathbb{R}^{n_y \times n_y}$ (number of measured states n_y). As a stability criterion for the Lyapunov function, the condition

$$[\dot{V}_{a,O}] - [\mathbf{e}]^T \cdot \mathbf{P}_O \mathbf{P}_O^{+} \mathbb{C}_O^T \mathbf{H}_s \cdot \mathrm{sign}\left([\mathbf{e}_m]\right) + \frac{1}{2}\mathrm{trace}\left\{\mathbf{G}^T \frac{\partial^2 V_O}{\partial \mathbf{e}^2}\mathbf{G}\right\} < -\mathbf{q}_O^T \left|[\mathbf{e}_m]\right| \tag{3.23}$$

with $[\mathbf{e}] = \left([\mathbf{x}] - [\hat{\mathbf{x}}]\right)$, where $[\mathbf{x}] = \mathbf{x} + [\Delta\mathbf{x}_c]$ and $[\hat{\mathbf{x}}] = \hat{\mathbf{x}} + [\Delta\mathbf{x}_e]$, as well as

$$[\dot{V}_{a,O}] = [\mathbf{e}]^T \mathbf{P}_O \cdot \left(\mathbb{A}_C \cdot [\mathbf{x}] + \mathbb{B}_C \cdot \mathbf{u} - \mathbb{A}_O \cdot [\hat{\mathbf{x}}] - \mathbb{B}_O \cdot \mathbf{u} - \mathbf{H}_p \cdot \left(\mathbf{y}_m - \hat{\mathbf{y}}_m + [\Delta\mathbf{y}_m]\right)\right) \tag{3.24}$$

hold (time arguments are omitted). As already explained for the sliding mode control design, the switching amplitudes are determined component-wise using the following cases to prevent a division by zero, where $[\delta_O]$ is a small interval around zero [17], according to

$$\mathbf{h}_s = \begin{cases} \mathbf{0}, & \text{if } \ [\delta_O] \subseteq [\mathbf{e}_m]^T\,[\mathbf{e}_m] \\ \sup\left(\left|[\mathbf{e}_m]\right|^{+} \cdot \left([\dot{V}_{a,O}] + \frac{1}{2} \cdot \mathrm{trace}\left\{\mathbf{G}^T \frac{\partial^2 V_O}{\partial \mathbf{e}^2}\mathbf{G}\right\}\right) + \mathbf{q}_O^T\right), & \text{else.} \end{cases} \tag{3.25}$$

The interval pseudo inverse is computed as $\left|[\mathbf{e}_m]\right|^{+} = \left(\left|[\mathbf{e}_m]\right|^T \left|[\mathbf{e}_m]\right|\right)^{-1} \cdot \left|[\mathbf{e}_m]\right|^T$ with the absolute value of the difference between measured and estimated states $\left|[\mathbf{e}_m]\right|$ of the corresponding interval $[\mathbf{e}_m]$ for each component i

$$\left|\left[e_{m,i}\right]\right| = \begin{cases} \left[-\overline{e}_{m,i}\ ;\ -\underline{e}_{m,i}\right] & \text{for } \overline{e}_{m,i} \le 0 \\ \left[\underline{e}_{m,i}\ ;\ \overline{e}_{m,i}\right] & \text{for } \underline{e}_{m,i} \ge 0 \\ \left[0\ ;\ \max\{|\underline{e}_{m,i}|, |\overline{e}_{m,i}|\}\right] & \text{else.} \end{cases} \tag{3.26}$$

As already described for the dual task of control in the ISMC, the interval $[\delta_O]$ in the ISMO is taken into consideration to reduce chattering and the calculated switching amplitude.

The following section illustrates the presented procedure for a cascaded sliding mode observer structure estimating not only non-measurable system states but also uncertain system parameters in combination with trajectory tracking by the ISMC.

4 Application Scenario: Simplified Model for the Longitudinal Dynamics of a Vehicle

The presented interval sliding mode controller and observer are used in the following for trajectory tracking and state as well as parameter estimation of a simplified model for the longitudinal dynamics of a vehicle. Assume this system is given by the state-space model $\mathbf{f}(\mathbf{x}(t), [\mathbf{p}], \mathbf{u}(t)) = \dot{\mathbf{x}}(t) = \left[\dot{x}_1(t),\ \dot{x}_2(t)\right]^T$ according to

$$\dot{\mathbf{x}}(t) = \mathbf{A} \cdot \mathbf{x}(t) + \mathbf{b} \cdot u(t) = \begin{bmatrix} 0 & 1 \\ 0 & \alpha \end{bmatrix} \begin{bmatrix} x_1(t) \\ x_2(t) \end{bmatrix} + \begin{bmatrix} 0 \\ \beta \end{bmatrix} u(t)$$
$$y(t) = x_1(t). \tag{4.1}$$

Two not a-priori known parameters $\alpha = -\frac{d}{m} \in [\alpha]$ and $\beta = \frac{1}{m} \in [\beta]$ with the mass m and the velocity-proportional friction coefficient d are included. Both parameters have a large influence on the system dynamics of the nonlinear model since they are coupled multiplicatively with the time-varying system states and the input. This is the reason, why it is important to estimate states and parameters both in a robust way. In general, it is assumed that the system parameters are located in the intervals $\alpha \in [\alpha] = -0.2 \cdot [-1; 1]$ and $\beta \in [\beta] = [0.9; 1.1]$.

Figure 3 illustrates the implementation. The task of trajectory tracking of the system is fulfilled by the ISMC. Since only the first state is measurable, it is necessary to estimate at least the second state as well which is done by the ISMO in subsystem S_1. Then, the estimates of S_1 are used as virtual measurements in ISMO subsystem S_2 to estimate the system parameters in a cascaded way. The approach is implemented using s-functions in Matlab/Simulink in combination with the C++ library C-XSC [20] and INTLAB [14]. For the calculation of the controller gain matrices of the linear model, additionally YALMIP [10] and SEDUMI [19] are used for solving LMIs according to Sect. 3.2 and [12].

Additionally, stochastic noise is considered which has different purposes. On the one hand, measurement noise reproduces the inaccuracy of measured data of the real application. On the other hand, process noise can be interpreted as a random disturbance to model for example discretization errors and friction, that influence a system but cannot be quantified easily.

4.1 Cascaded Interval Sliding Mode Observer

The interval-based sliding mode observer has a cascaded structure. The reason is, that in general states change faster than parameters, since the states are time-varying whereas parameters such as masses are assumed to be constant.

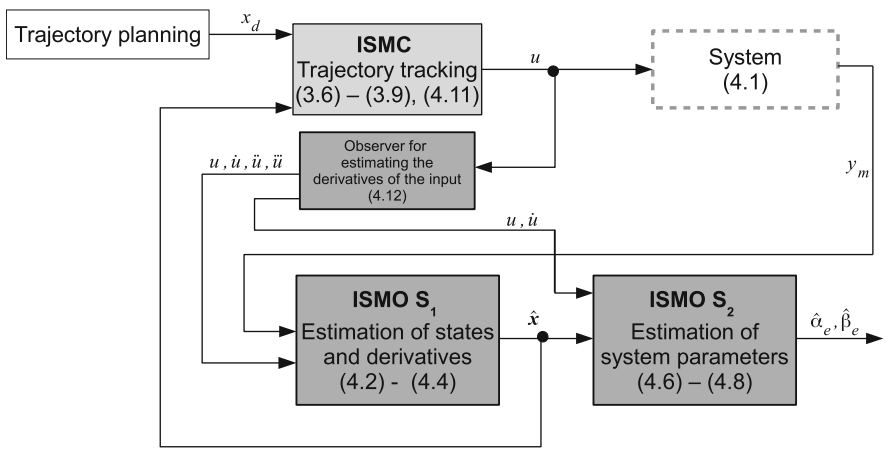

Fig. 3 Block diagram of the illustrative example

Typically, parameters and state variables are coupled, as for example the friction force that depends here on the second state x_2, which can be interpreted as velocity.

The subsystem S_1 estimates the states up to the fourth time derivative of the position x_1 using an integrator chain with the output x_1 in the parallel model. The model of the observer subsystem S_1 is given by

$$\mathbf{f}^{(S_1)} = \begin{bmatrix} \dot{x}_1 \\ \dot{x}_2 \\ \dot{x}_3 \\ \dot{x}_4 \\ \dot{z}_1 \end{bmatrix} = \begin{bmatrix} x_{2,d} + \left[\Delta x_{c,2}^{(S_1)}\right] \\ [\alpha]\left(x_{2,d} + \left[\Delta x_{c,2}^{(S_1)}\right]\right) + [\beta]u \\ [\alpha]^2\left(x_{2,d} + \left[\Delta x_{c,2}^{(S_1)}\right]\right) + [\alpha][\beta]u + [\beta]\dot{u} \\ [\alpha]^3\left(x_{2,d} + \left[\Delta x_{c,2}^{(S_1)}\right]\right) + [\alpha]^2[\beta]u + [\alpha][\beta]\dot{u} + [\beta]\ddot{u} \\ [\alpha]^4\left(x_{2,d} + \left[\Delta x_{c,2}^{(S_1)}\right]\right) + [\alpha]^3[\beta]u + [\alpha]^2[\beta]\dot{u} + [\alpha][\beta]\ddot{u} + [\beta]\dddot{u} \end{bmatrix} \tag{4.2}$$

with the output $y_m^{(S_1)} = x_1$ and the desired trajectory for the second system state $x_{2,d}$, because the real state x_2 is not directly measurable. The corresponding observer parallel model can be expressed by an integrator chain according to

$$\hat{\mathbf{f}}^{(S_1)} = \begin{bmatrix} \dot{\hat{x}}_1 \\ \dot{\hat{x}}_2 \\ \dot{\hat{x}}_3 \\ \dot{\hat{x}}_4 \\ \dot{\hat{z}}_1 \end{bmatrix} = \begin{bmatrix} \hat{x}_2 + \left[\Delta x_{e,1}^{(S_1)}\right] \\ \hat{x}_3 + \left[\Delta x_{e,2}^{(S_1)}\right] \\ \hat{x}_4 + \left[\Delta x_{e,3}^{(S_1)}\right] \\ \hat{z}_1 + \left[\Delta x_{e,4}^{(S_1)}\right] \\ 0 + \left[\Delta x_{e,5}^{(S_1)}\right] \end{bmatrix}. \tag{4.3}$$

The derivatives of the system input $\dot{u} = \dot{\hat{u}}$, $\ddot{u} = \ddot{\hat{u}}$ and $\dddot{u} = \dddot{\hat{u}}$ and the input $u = \hat{u}$ itself result from an observer that represents an integrator chain for the system input (see Sect. 4.3) in order to provide smooth derivatives of the input. The interval sliding mode observer for subsystem S_1 is then given by

$$\dot{\hat{\mathbf{x}}}^{(S_1)} = \underbrace{\begin{bmatrix} 0\,1\,0\,0\,0 \\ 0\,0\,1\,0\,0 \\ 0\,0\,0\,1\,0 \\ 0\,0\,0\,0\,1 \\ 0\,0\,0\,0\,0 \end{bmatrix}}_{\mathbf{A}_O^{(S_1)}} \underbrace{\begin{bmatrix} \hat{x}_1 \\ \hat{x}_2 \\ \hat{x}_3 \\ \hat{x}_4 \\ \hat{z}_1 \end{bmatrix}}_{\hat{\mathbf{x}}^{(S_1)}} + \mathbf{H}_p^{(S_1)} \cdot [e_m^{(S_1)}] + \mathbf{P}_O^{(S_1)+}\mathbf{C}_O^{(S_1)}\mathbf{H}_s^{(S_1)} \cdot \operatorname{sign}([e_m^{(S_1)}]), \tag{4.4}$$

with the definition of the sign function in analogy to Eq. (3.18) and $[e_m^{(S_1)}] = e_m^{(S_1)} - [\Delta y_m]$ with $e_m^{(S_1)} = x_1 + \hat{x}_1$. The matrices for the stabilization of the linear part are $\mathbf{H}_p^{(S_1)}$ (determined by pole placement) and $\mathbf{P}_O^{(S_1)}$. Note, since subsystem 1 has only one output $y^{(S_1)} = x_1$, the matrix $\mathbf{H}_p^{(S_1)}$ becomes a vector and the switching term $\mathbf{H}_s^{(S_1)} \cdot \operatorname{sign}([e_m^{(S_1)}])$ scalar. The matrix $\mathbf{P}_O^{(S_1)}$ results from solving the associated Lyapunov equation according to

$$\tilde{\mathbf{A}}_O^{(S_1)} \cdot \mathbf{P}_O^{(S_1)} + \mathbf{P}_O^{(S_1)} \cdot \tilde{\mathbf{A}}_O^{(S_1)T} + \mathbf{Q}^{(S_1)} = \mathbf{0} \tag{4.5}$$

with $\tilde{\mathbf{A}}_O^{(S_1)} = \mathbf{A}_O^{(S_1)} - \mathbf{H}_p^{(S_1)} \cdot \mathbf{C}_O^{(S_1)}$.

Subsystem S_2 estimates the system parameters and states using integrator disturbance models for the parameters. The model of subsystem S_2 is defined by

$$\mathbf{f}^{(S_2)} = \begin{bmatrix} \dot{x}_2 \\ \dot{x}_3 \\ \dot{\alpha}_e \\ \dot{\beta}_e \\ \dot{z}_2 \end{bmatrix} = \begin{bmatrix} [\alpha]\left(x_2 + \left[\Delta x_{c,1}^{(S_2)}\right]\right) + [\beta]u + \left(z_2 + \left[\Delta x_{c,5}^{(S_2)}\right]\right) \\ [\alpha]^2\left(x_2 + \left[\Delta x_{c,1}^{(S_2)}\right]\right) + [\alpha][\beta]u + [\beta]\dot{u} \\ 0 + \left[\Delta x_{c,3}^{(S_2)}\right] \\ 0 + \left[\Delta x_{c,4}^{(S_2)}\right] \\ 0 + \left[\Delta x_{c,5}^{(S_2)}\right] \end{bmatrix} \tag{4.6}$$

with the point-valued parameter estimates α_e and β_e, that are estimated by this subsystem. The state x_2 is now the second state provided by subsystem S_1. The output vector is defined as $\mathbf{y}_m^{(S_2)} = [x_2,\ x_3,\ z_2]^T$. Under the assumption that the model error is slowly varying for S_2, the parallel model is described by

$$\hat{\mathbf{f}}^{(S_2)} = \begin{bmatrix} \dot{\hat{x}}_2 \\ \dot{\hat{x}}_3 \\ \dot{\hat{\alpha}}_e \\ \dot{\hat{\beta}}_e \\ \dot{\hat{z}}_2 \end{bmatrix} = \begin{bmatrix} [\delta_\alpha] \cdot \left(\hat{x}_2 + \left[\Delta x_{e,1}^{(S_2)}\right]\right) + [\delta_\beta]u + \left(\hat{z}_2 + \left[\Delta x_{e,5}^{(S_2)}\right]\right) \\ [\delta_\alpha]^2 \cdot \left(\hat{x}_2 + \left[\Delta x_{e,1}^{(S_2)}\right]\right) + [\delta_\alpha][\delta_\beta]u + [\delta_\beta]\dot{u} \\ 0 + \left[\Delta x_{e,3}^{(S_2)}\right] \\ 0 + \left[\Delta x_{e,4}^{(S_2)}\right] \\ 0 + \left[\Delta x_{e,5}^{(S_2)}\right] \end{bmatrix} \tag{4.7}$$

with the enlarged intervals for the two estimated parameters $[\delta_\alpha] = \left([\alpha] + \left[\Delta x_{e,3}^{(S_2)}\right]\right)$ and $[\delta_\beta] = \left([\beta] + \left[\Delta x_{e,4}^{(S_2)}\right]\right)$.

The interval sliding mode observer for the subsystem S_2 follows as

$$\dot{\hat{\mathbf{x}}}^{(S_2)} = \underbrace{\begin{bmatrix} 0 & 0 & x_{2,w} & 0 & 1 \\ \alpha_O^2 & 0 & 0 & \dot{u}_w & 0 \\ 0 & 0 & 0 & 0 & 0 \\ 0 & 0 & 0 & 0 & 0 \\ 0 & 0 & 0 & 0 & 0 \end{bmatrix}}_{\mathbf{A}_O^{(S_2)}} \underbrace{\begin{bmatrix} \hat{x}_2 \\ \hat{x}_3 \\ \hat{\alpha}_e \\ \hat{\beta}_e \\ \hat{z}_2 \end{bmatrix}}_{\hat{\mathbf{x}}^{(S_2)}} + \underbrace{\begin{bmatrix} \beta_e \\ \alpha_e \cdot \beta_e \\ 0 \\ 0 \\ 0 \end{bmatrix}}_{\mathbf{b}_O^{(S_2)}} \cdot u + \mathbf{H}_p^{(S_2)} \cdot [\mathbf{e}_m^{(S_2)}] + \mathbf{P}_O^{(S_2)+} \mathbf{C}_O^{(S_2)} \mathbf{H}_s^{(S_2)} \cdot \operatorname{sign}([\mathbf{e}_m^{(S_2)}]) \tag{4.8}$$

with $[\mathbf{e}_m^{(S_2)}] = \mathbf{e}_m^{(S_2)} + [\Delta \mathbf{y}_m^{(S_2)}]$ and $\mathbf{e}_m^{(S_2)} = (\mathbf{y}_m^{(S_2)} - \hat{\mathbf{y}}_m^{(S_2)}) = \left[x_2 - \hat{x}_2,\ x_3 - \hat{x}_3,\ 0 - \hat{z}_2\right]^T$. The matrices $\mathbf{H}_p^{(S_2)}$ and $\mathbf{P}_O^{(S_2)}$ stabilize the linear part of the observer ordinary differential equations. For subsystem S_2, the switching term $\mathbf{H}_s^{(S_2)} \cdot \operatorname{sign}(\mathbf{e}_m^{(S2)} + [\Delta \mathbf{y}_m^{(S_2)}])$ has three components. The working set point is defined as $x_{2,w} = 4$, $\dot{u}_w = 5$, and $\alpha_O = -0.15 \in [\alpha]$.

Note, that the switching amplitudes for both subsystems are calculated separately according to Sect. 3.4. For that purpose, the definition of the continuous part of the time derivative of the Lyapunov function candidates for both subsystems introduced in (3.24), needs to be slightly adapted, since the models of both observers (4.2) and (4.6) are nonlinear. Therefore, the expression (3.24) is reformulated according to

$$[\dot{V}_{a,O,k}] = [\mathbf{e}] \cdot \mathbf{P}_O^{(k)} \cdot ([\mathbf{f}^{(k)}] - [\hat{\mathbf{f}}^{(k)}] - \mathbf{H}_p^{(k)} \cdot \mathbf{e}_m^{(k)}), \tag{4.9}$$

with $k \in \{S_1, S_2\}$.

In subsystem S_1, it is assumed that the measurement of the state x_1 is corrupted by measurement noise with a standard deviation of $\mathbf{G}_m^{(S_1)} =: G_m^{(S_1)} = 0.05$, where the process noise is taken into consideration only in the calculation of the trace with $\mathbf{G}_p^{(S_1)} = [0\ 0\ 0\ 0\ 0.5]^T$. Subsystem S_2 contains the stochastic disturbances of process

and measurement noise according to

$$\mathbf{G}_p^{(S_2)} = \begin{bmatrix} 0 & 0 & 0 & 0 & 0 \\ 0 & 0 & 0 & 0 & 0 \\ 0 & 0 & 0.2 & 0 & 0 \\ 0 & 0 & 0 & 0.3 & 0 \\ 0 & 0 & 0 & 0 & 0.5 \end{bmatrix} \quad \text{and} \quad \mathbf{G}_m^{(S_2)} = \begin{bmatrix} 0.5 & 0 & 0 \\ 0 & 0.2 & 0 \\ 0 & 0 & 0.7 \end{bmatrix} \tag{4.10}$$

in the corresponding calculation of the trace T. The stability margins are defined as $q_O^{(S_1)} = 0$ and $\mathbf{q}_O^{(S_2)} = [50\ ,\ 50\ ,\ 50]^T$. The control and estimation intervals are chosen as $[\Delta x_{c,j}^{(S_1)}] = [-0.5\ ;\ 0.5]$, $[\Delta x_{e,j}^{(S_1)}] = [-2\ ;\ 2]$, component-wise, for S_1 and $[\Delta x_{c,j}^{(S_2)}] = [-1\ ;\ 1]$, $[\Delta x_{e,j}^{(S_2)}] = [-5\ ;\ 5]$, component-wise, for S_2 and all $j \in \{1, ..., 5\}$.

The measurement error intervals are defined by $[\Delta y_m^{(S_1)}] = [-0.05\ ;\ 0.05]$ and $[\Delta \mathbf{y}_m^{(S_2)}] = [[-0.1\ ;\ 0.1], [-0.1\ ;\ 0.1], [-10^{-6}\ ;\ 10^{-6}]]^T$.

4.2 Interval Sliding Mode Controller

The purpose of the sliding mode controller is to obtain perfect trajectory tracking in the optimal case. Therefore, desired trajectories for $x_{1,d}$, $x_{2,d}$ and $x_{3,d}$ are specified. The task of the controller is to minimize the difference between the first two components of the desired trajectory and the corresponding estimated states from the observer subsystem S_1 according to $\tilde{\mathbf{x}} = \mathbf{x}_d - \hat{\mathbf{x}} = \mathbf{0}$. Selecting these two components coincides with the fact that the system is described by the state-space representation (4.1) of order $n = 2$. The ISMC can be described using the following definitions

$$\mathbf{A}_C = \begin{bmatrix} 0 & 1 \\ 0 & \alpha_C \end{bmatrix}, \mathbf{B}_C = \begin{bmatrix} 0 \\ \beta_C \end{bmatrix}, \mathbf{C}_C = \begin{bmatrix} 1 & 0 \end{bmatrix} \tag{4.11}$$

with the point-valued parameters $\alpha_C = -0.2 \in [\alpha]$ and $\beta_C = 1 \in [\beta]$ and the covariance matrices $\mathbf{G}_p = \begin{bmatrix} 0.01 & 0 \\ 0 & 0.7 \end{bmatrix}$, $\mathbf{G}_m =: G_m = 0.05$ as well as the stability margin $\mathbf{q}_C = [10\ ,\ 10]^T$ for both states. Moreover, the control error interval vector is defined by $[\Delta \mathbf{x}_c] = [[-0.5\ ;\ 0.5]\ ,\ [-0.5\ ;\ 0.5]]^T$. The matrices $\mathbf{K}$ and $\mathbf{P}_C$ for the stabilization of the linear part of the system are defined by LMIs, see Sect. 3.2.

4.3 Observer for the System Input

The goal of this observer is to estimate the derivatives of the system input provided by the ISMC in such a way that sufficiently smooth trajectories are obtained. These derivatives are necessary for the system descriptions of the cascaded observer in the previous subsection. Currently, the observer relies on an integrator chain according to

$$\underbrace{\begin{bmatrix} \dot{\hat{u}} \\ \ddot{\hat{u}} \\ \dddot{\hat{u}} \\ \hat{u}^{(4)} \\ \dot{z}_u \end{bmatrix}}_{\dot{\hat{\mathbf{x}}}_\mathbf{u}} = \underbrace{\begin{bmatrix} 0 & 1 & 0 & 0 & 0 \\ 0 & 0 & 1 & 0 & 0 \\ 0 & 0 & 0 & 1 & 0 \\ 0 & 0 & 0 & 0 & 1 \\ 0 & 0 & 0 & 0 & 0 \end{bmatrix}}_{\hat{\mathbf{A}}_u} \cdot \underbrace{\begin{bmatrix} \hat{u} \\ \dot{\hat{u}} \\ \ddot{\hat{u}} \\ \dddot{\hat{u}} \\ z_u \end{bmatrix}}_{\hat{\mathbf{x}}_u} + \mathbf{H}_u \cdot (u - \hat{u}), \tag{4.12}$$

where the column vector $\mathbf{H}_u$ is computed by linear quadratic estimator design so that (4.12) has properties that are similar to a continuous Kalman Filter. Then, the estimates of the vector $\hat{\mathbf{x}}_u$ are used as the input u and its three derivatives $\dot{u}$, $\ddot{u}$ and $\dddot{u}$ within the observer models of S_1 and S_2.

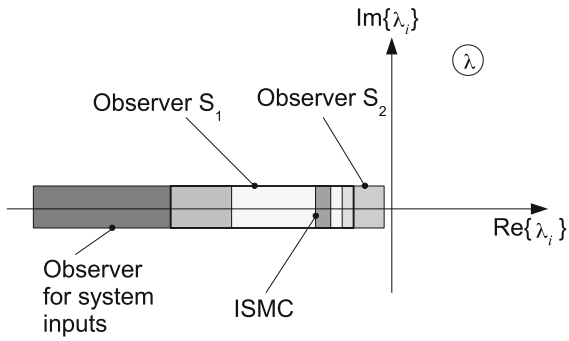

Fig. 4 Location of the eigenvalues λ_i of the controller and the observers

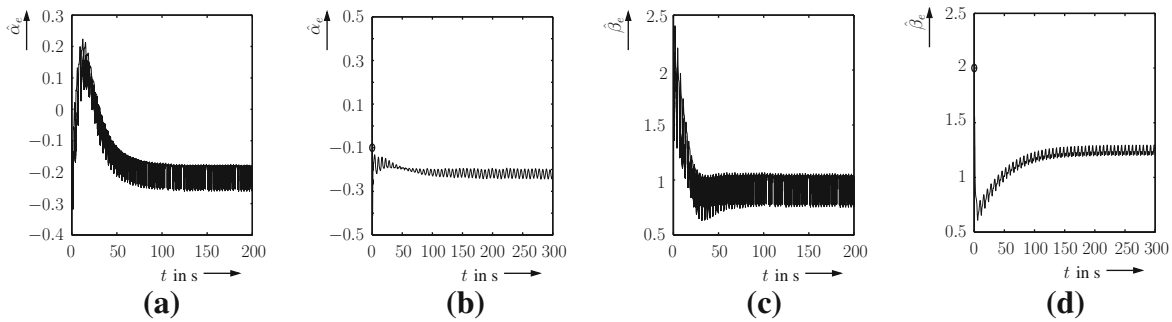

Fig. 5 Estimation results of the system parameters $\hat{\alpha}_e$ and $\hat{\beta}_e$ for scenario 1 (without closed-loop control) and 2 (with closed-loop control). **a** Estimate $\hat{\alpha}_e$ (scenario 1), **b** estimate $\hat{\alpha}_e$ (scenario 2), **c** estimate $\hat{\beta}_e$ (scenario 1), **d** estimate $\hat{\beta}_e$ (scenario 2)

4.4 Simulation Results of Control as well as State and Parameter Estimation

In the following, simulation results are shown for two scenarios. Scenario 1 includes only an open-loop control for the cascaded observer without stochastic disturbances but with bounded parameter intervals. Scenario 2 is implemented using the described closed-loop control (ISMC) as well as the cascaded observer structure with stochastic and bounded disturbances. For the presented results, the real parts of the eigenvalues $\mathrm{Re}\{\lambda_i\}$ of all components of the closed-loop control and estimation for the application scenario have been chosen according to Fig. 4.

For the first scenario, the estimation results of the two system parameters according to [16] are depicted in Fig. 5 in comparison with the estimates that result from the closed-loop control in the second scenario. As it can be seen, the estimate $\hat{\alpha}_e$ with closed-loop control is better although stochastic disturbances are considered. Especially, the parameter $\hat{\alpha}_e$ in Scenario 1 changes the sign which might compromise the systems stability at the begin of the simulation if the parameter was used in an adaptive closed-loop feedback control. The results show, that chattering can be reduced to approx 50 % by using a closed-loop control considering stochastic disturbances. Therefore, all following results represent scenario 2.

The standard deviation of the process noise with a value of $\sigma = \mathbf{G}_{p,2,2} = 0.7$, which can be interpreted as additive uncertainty on the actor dynamics in the second system state, corresponds to a disturbance with the range of approx. $3 \cdot \sigma \cdot [-1\,;\ 1] = [-2.1\,;\ 2.1]$. As it can be seen in Fig. 6, this is a large impact on the system dynamics in the second equation of the state-space representation according to Eqs. (3.6) and (4.1). The corresponding control and estimation errors for both system states are depicted in Fig. 7. Due to the large impact of the process noise, it has to be pointed out that the presented procedure is robust against disturbances.

In Fig. 8, the dependencies between the switching amplitudes and the estimation error intervals for the position (difference between the first system state and the first state of subsystem S_1) and the velocity (difference between

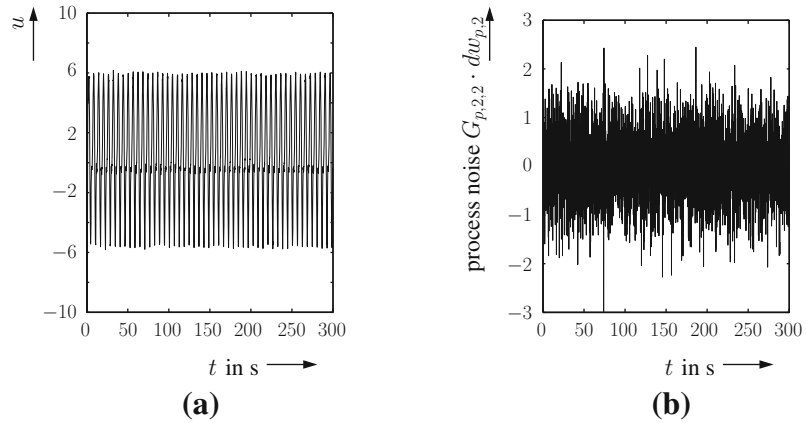

Fig. 6 Feedback control signal (3.9) and stochastic disturbance in the second state equation. **a** System input u provided by ISMC, **b** process noise influencing the second system state in (4.1)

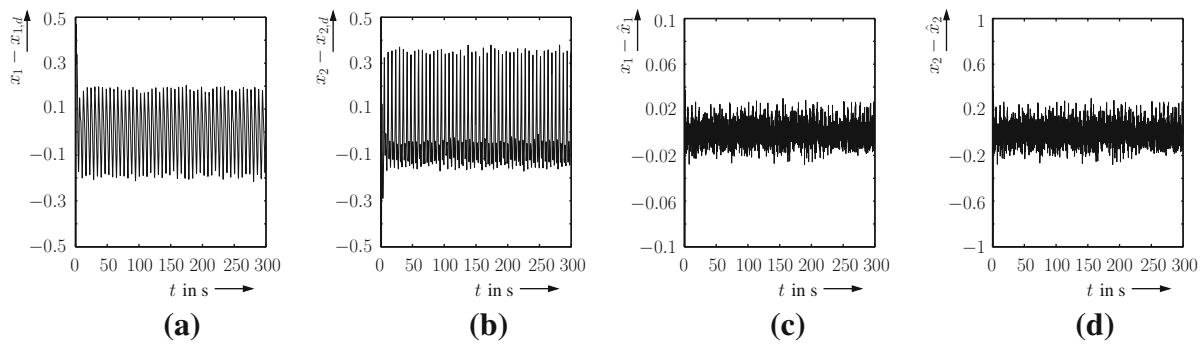

Fig. 7 Estimation errors (scenario 2). **a** Control error $x_1 - x_{1,d}$, **b** control error $x_2 - x_{2,d}$, **c** estimation error $x_1 - \hat{x}_1$, **d** estimation error $x_2 - \hat{x}_2$

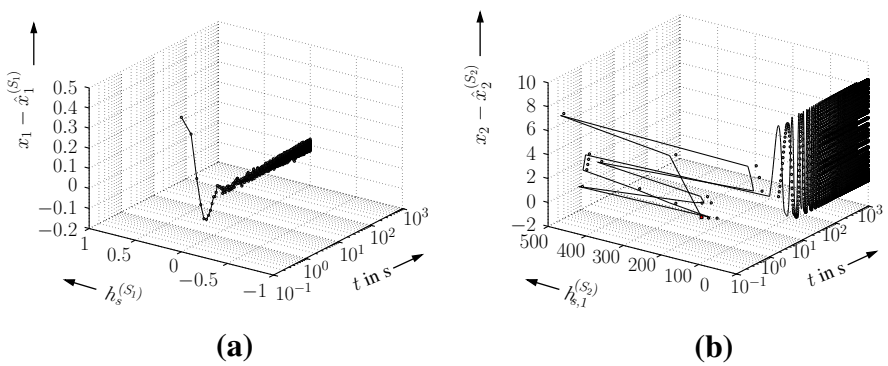

Fig. 8 Relation between the switching amplitudes of the cascaded observer and the corresponding estimation errors. **a** Estimation error $x_1 - \hat{x}_1$, **b** estimation error $x_2 - \hat{x}_2$

the second system state and the first state of subsystem S_2) are shown.[3] It can be seen that the switching amplitudes at the begin of the simulation are not equal to zero. At these points, the corresponding variable structure components are active, since the sign of the estimation error can be determined unambiguously. From 1 s (left) and 10 s (right), resp., the estimation errors are too small to determine the sign of the estimation errors for the sliding mode observers.

[3] Due to interval uncertainty, the sliding surface is generalized to a sliding area by the presented control and observer approaches.

This is the reason, why the switching amplitudes are then set to zero in order to avoid a possible division by zero according in Eq. (3.25). As it can be seen from Fig. 8, the switching amplitudes are significantly smaller in the near surrounding area of the sliding surfaces of the sliding mode observer for both subsystems. This feature is realized by the small interval $[\delta_O]$ in Sect. 3.4. In contrast to this effect, it is well known that in classical sliding mode approaches the switching amplitude influences the system as long as the sliding surface is not exactly reached.

5 Conclusions and Outlook on Future Work

In this paper, sliding mode techniques have been extended such that intervals for bounded uncertainty as well as stochastic disturbances are considered to develop robust control and estimation strategies guaranteeing asymptotic stability of the system. In future work, the stabilization of the continuous parts for control and estimation will be performed simultaneously to achieve a joint stability proof of the system using a single Lyapunov function. Moreover, the dynamic feedforward control in the control law (3.9) needs to be adapted in order to use estimated variations of the parameters. Additionally, a strategy should be considered, that prevents under all circumstances the system parameters from changing their a-priori unknown sign as it occurred using the cascaded observer without a closed-loop control. The most important point is, to validate the presented closed-loop control on a test rig, that is available at the Chair of Mechatronics at the University of Rostock, as it has already been done for the open-loop control in [15].

References

1. Åström, K.J.: Introduction to stochastic control theory. In: Mathematics in Science and Engineering. Academic Press, London (1970)
2. Balakrishnan, V., Vandenberghe, L.: Semidefinite programming duality and linear time-invariant systems. IEEE Trans. Autom. Control **48**(1), 30–41 (2003)
3. Barmish, B.R.: New Tools for Robustness of Linear Systems. Macmillan, New York (1994)
4. Bartoszewicz, A., Nowacka-Leverton, A.: Time-Varying Sliding Modes for Second and Third Order Systems. In: Lecture Notes in Control and Information Sciences, vol. 382. Springer-Verlag, New York (2009)
5. Dötschel, Th., Rauh, A., Aschemann, H.: Reliable Control and Disturbance Rejection for the Thermal Behavior of Solid Oxide Fuel Cell Systems. In: Paper presented at MATHMOD 2012, Vienna (2012)
6. Engell, S.: Entwurf nichtlinearer Regelungen. R. Oldenbourg Verlag, München (in German) (1995)
7. Fridman, L., Moreno, J., Iriarte, R.: Sliding Modes After the First Decade of the 21st Century: State of the Art. In: Lecture Notes in Control and Information Sciences, vol. 412 (2011)
8. Jaulin, L., Kieffer, M., Didrit, O., Walter, É.: Applied Interval Analysis. Springer-Verlag, London (2001)
9. Kushner, H.: Stochastic Stability and Control. Academic Press, New York (1967)
10. Löfberg, J.: YALMIP: A Toolbox for Modeling and Optimization in MATLAB. In: Proceedings of IEEE International Symposium on Computer Aided Control Systems Design, pp. 284–289, Taipei (2004)
11. Rauh, A., Aschemann, H.: Interval-based sliding mode control and state estimation for uncertain systems. In Proceedings of IEEE International Conference on Methods and Models in Automation and Robotics, Miedzyzdroje (2012)
12. Rauh, A., Dittrich, Ch., Aschemann, H., Nedialkov, N.S., Pryce, J.D.: A differential-algebraic approach for robust control design and disturbance compensation of finite-dimensional models of heat transfer processes. In: Proceedings of the IEEE International Conference on Mechatronics ICM 2013, Vicenza (2013)
13. Rauh, A., Gebhardt, J., Aschemann, H.: Guaranteed stabilizing control strategies for boom cranes in marine applications. In: Proceedings of the 2nd International Conference on Control and Fault-Tolerant Systems, SysTol'13, Nice (2013)
14. Rump, S.M.: INTLAB—INTerval LABoratory. In: Csendes, T. (Ed.) Developments in Reliable Computing, pp. 77–104. Kluwer Academic Publishers, Dordrecht. http://www.ti3.tu-harburg.de/rump/intlab/ (1999). Accessed July 2014
15. Senkel, L., Rauh, A., Aschemann, H.: Optimal Input Design for Online State and Parameter Estimation using Interval Sliding Mode Observers. In Proceedings of 52nd IEEE Conference on Decision and Control, CDC, Florence (2013)
16. Senkel, L., Rauh, A., Aschemann, H.:Interval-based sliding mode observer design for nonlinear systems with bounded measurement and parameter uncertainty. In: Proceedings of the IEEE International Conference on Methods and Models in Automation and Robotics, MMAR 2013, Miedzyzdroje (2013)
17. Senkel, L., Rauh, A., Aschemann, H.: Robust sliding mode techniques for control and state estimation of dynamic systems with bounded and stochastic uncertainty. In: Second International Conference on Vulnerability and Risk Analysis and Managemet 2014, ICVRAM 2014 (to appear). (2014)

18. Shtessel, Y., Edwards, Ch., Fridman, L., Levant, A. (eds). Sliding Mode Control and Observation, 1st edn. Springer Series, Birkhäuser, Basel (2014)
19. Sturm, J.F.: Using SeDuMi 1.02, a MATLAB toolbox for optimization over symmetric cone. Optim. Methods Softw. **11–12**(1–4), 625–653 (1999)
20. Universität Karlsruhe (Institut für Angewandte Mathematik, Forschungsschwerpunkt CAVN), Universität Wuppertal (Wissenschaftliches Rechnen/Softwaretechnologie): C-XSC—a C++ class library. http://www2.math.uni-wuppertal.de/~xsc/xsc/cxsc.html (2007). Accessed July 2014
21. Utkin, V.I.: Sliding Modes in Control and Optimization. Springer-Verlag, Berlin (1992)
22. Utkin, V.I.: Sliding Mode Control Design Principles and Applications to Electric Drives. IEEE Trans. Ind. Electron. **40**(1), 23–36 (1993)